

EXTRASYNAPTIC transmission is mediated by the diffusion of transmitters, through the extracellular space (ECS) to receptors on neurons and glia. The three-dimensional diffusion of tetramethylammonium (mol. wt 74.1 kDa) was investigated in the isolated rat spinal cord at postnatal days 4–20. The diffusion parameters of the ECS, volume fraction  $\alpha$ , tortuosity  $\lambda$  ( $\lambda^2 = \text{free/apparent diffusion coefficient in tissue}$ ) and nonspecific uptake  $k'$ , were different in gray and white matter. In both gray and white matter,  $\alpha$  decreased with neuronal development and gliogenesis by about 15% while  $\lambda$  significantly increased. Diffusion in gray matter remained isotropic ( $\lambda = 1.65$ ), while in white matter it became anisotropic, i.e. easier along the fibers ( $\lambda = 1.38$ ) than across the fibers ( $\lambda = 1.80$ ). Anisotropy increased in the second postnatal week, during pronounced myelination. In myelinated tissue, preferential diffusion of neuroactive substances occurs along the axons.

**Key words:** Apparent diffusion coefficient; Diffusion-weighted NMR; Extracellular space; Extracellular volume; Extrasynaptic transmission; Myelin; Tortuosity

## Heterogeneous and anisotropic diffusion in the developing rat spinal cord

Šárka Prokopová, Lýdia Vargová and Eva Syková<sup>CA</sup>

Department of Neuroscience, Institute of Experimental Medicine AS CR, Vídeňská 1083, Prague 142 20; Department of Neuroscience, 2nd and 3rd Medical Faculties, Charles University, V úvalu 84, Prague 150 18, Czech Republic

<sup>CA</sup>Corresponding Author

### Introduction

There is increasing evidence that extrasynaptic transmission, mediated by the diffusion of neuroactive substances (including ions, transmitters and other macromolecules) through the extracellular space (ECS), plays a role in short- and long-distance communication between neurons, axons and glia.<sup>1,2</sup> It is, therefore, of interest to study the diffusion of substances of various sizes through the ECS. It has been previously shown that small cations, such as tetraethylammonium (TEA<sup>+</sup>) or tetramethylammonium (TMA<sup>+</sup>), move through the ECS of the rat brain and spinal cord in a similar manner as do neutral dextrans of mol. wt 3000 and 10 000.<sup>3</sup> By diffusing through the ECS, transmitters and neuromodulators can reach high-affinity receptors located outside synapses on neuronal elements as well as on glial cells (for review see Ref. 4). This type of extrasynaptic transmission is also called volume transmission,<sup>5</sup> as the neuroactive substances and ions move (diffuse) through the volume of the ECS.

The size, structure and composition of the ECS determine the migration of substances in the brain.<sup>2</sup> There is anatomical evidence that glial cells are not randomly arranged, but are in a precise anatomic relationship with neurons and axons.<sup>6</sup> In principle, the structure of cellular aggregates, maturation and organization of glia and/or extracellular matrix can channel the migration of molecules in the ECS, so that diffusion in certain regions is anisotropic, i.e.

is facilitated in one direction rather than another. This would confer a certain degree of specificity to extrasynaptic transmission. To study diffusion anisotropy in the ECS, we measured TMA<sup>+</sup> diffusion in the rat spinal cord gray and white matter during the first three postnatal weeks. During this period there is extensive neuronal development and gliogenesis. As TMA<sup>+</sup> diffuses in all directions, we measured it independently in three orthogonal axes ( $x$ ,  $y$ ,  $z$ ).<sup>7,8</sup> The  $x$  axis lies along the axons; the  $y$  axis and  $z$  axis lie across the axons in the white matter (ventral funiculus). We addressed the question of whether anisotropic diffusion of substances occurs in the spinal cord ECS and how it is related to gliogenesis and myelination. Diffusion anisotropy in spinal cord has not been studied previously, yet it is critical for extrasynaptic transmission and MRI interpretation.<sup>2</sup>

### Materials and Methods

Experiments were performed on rat pups (Wistar strain) from P4 to P20 (date of birth taken as P0). After decapitation under ether anesthesia, spinal cords were isolated in a chamber with cold (8°C) artificial cerebrospinal fluid (ACF) of the following composition (in mM): NaCl 117.0, KCl 3.0, NaHCO<sub>3</sub> 35.0, Na<sub>2</sub>HPO<sub>4</sub> 1.25, D-glucose 10.0, sodium ascorbate 0.2, thiourea 0.2, MgCl<sub>2</sub> 1.3, CaCl<sub>2</sub> 1.5. The ascorbate and thiourea served as intra- and extracellular antioxidants and were added to the medium to minimize edema in spinal cord *in vitro*.<sup>9</sup>

The solution was saturated with 95% O<sub>2</sub> and 5% CO<sub>2</sub> (pH about 7.4). The isolated spinal cord was placed in a small chamber, and the preparation continuously perfused with ACF containing 0.1 mM tetramethylammonium chloride at a high perfusion rate of 10 ml/min. Over the course of 1 h the temperature was increased from 8 to 20–22°C. The measured values of the extracellular space volume fraction remained stable for more than 2 h *in vitro*, indicating a lack of cellular swelling due to ischemia-evoked metabolic stress.

The real-time iontophoretic method using TMA<sup>+</sup>-selective microelectrodes<sup>10</sup> was used to determine the volume of the ECS, the so-called extracellular space volume fraction  $\alpha$  ( $\alpha = \text{ECS volume}/\text{total tissue volume}$ ), and the tortuosity factor ( $\lambda$ ) that describes how the migration of molecules is slowed down by pore size, shape and connectivity. Tortuosity describes the geometry of the ECS and is calculated from the measured TMA<sup>+</sup> diffusion coefficients as  $\lambda = (D/ADC)^{0.5}$ , where  $D$  is the free diffusion coefficient and  $ADC$  is the apparent diffusion coefficient of TMA<sup>+</sup> in spinal cord.

TMA<sup>+</sup>-selective microelectrodes (TMA<sup>+</sup>-ISM) were used to measure TMA<sup>+</sup> diffusion parameters in the ECS. They were prepared as described previously.<sup>8,11,12</sup> The ion-sensing barrel contained ion-exchanger Corning 477317 and was back-filled with 100 mM TMA chloride. Electrodes were calibrated before and after each experiment in a sequence of solutions of 150 mM NaCl and 3 mM KCl with the addition of the following concentrations of TMA chloride (mM): 0.0003, 0.001, 0.003, 0.01, 0.03, 0.1, 0.3, 1.0, 3.0, 10.0.

For diffusion measurements, iontophoresis pipettes were prepared from glass tubes with the shank bent before back-filling with 0.5 M TMA chloride so that it could be aligned parallel to the TMA<sup>+</sup>-ISM (Fig. 1). Electrode arrays were made by gluing together TMA<sup>+</sup>-ISM and an iontophoresis pipette, with a tip separation of 100–220  $\mu\text{m}$ . After making a measurement in the  $x$  axis, the electrode was withdrawn from the spinal cord, rotated 90° and reinserted within 150  $\mu\text{m}$  of the original insertion point in order to make a measurement in the  $y$  axis. Measurements in the  $z$  axis were made using different electrode arrays with tips separated in the vertical plane by 100–220  $\mu\text{m}$ . The iontophoresis parameters were +20 nA bias current (continuously applied to maintain a constant transport number) with a +80 nA current step of 60 s duration to generate the diffusion curve. The indifferent electrode was Ag/AgCl wire placed in the bath. Potentials recorded on the reference barrel of the ISM were subtracted from the ion-selective barrel voltage measurements by means of buffer and subtraction amplifiers. Equations

describing the expected extracellular TMA<sup>+</sup> concentration,  $C$ , generated by iontophoresis in an anisotropic medium have been derived by Rice *et al.*<sup>7</sup> and used in our previous study.<sup>12</sup> The equations describe the change in  $C$  with time at a given separation between the iontophoresis and recording pipettes in the rectangular Cartesian coordinates,  $x$ ,  $y$  and  $z$ . The diffusion parameters describing the extracellular volume fraction,  $\alpha$ , the tortuosity along the three axes,  $\lambda_x$ ,  $\lambda_y$ ,  $\lambda_z$ , and non-specific uptake,  $k'$ , were determined by fitting the TMA<sup>+</sup> concentration curves using a non-linear curve-fitting simplex algorithm in the program VOLTORO (kindly provided by C. Nicholson).

Concentration *vs* time curves for TMA<sup>+</sup> diffusion were first recorded in 0.3% agar gel (Difco, Detroit) made up in a solution of 150 mM NaCl, 3 mM KCl and 1 mM TMA<sup>+</sup>, where  $\alpha = 1$ ,  $\lambda = 1$  and  $k' = 0$ . A non-linear curve-fitting simplex algorithm, implemented in the program VOLTORO, was used in order to determine the transport number ( $n$ ) of the iontophoresis micropipette and  $D$  for TMA<sup>+</sup>. After determining  $n$  in agar gel, measurements were made in the spinal cord to obtain ECS diffusion parameters  $\alpha$ ,  $\lambda_x$ ,  $\lambda_y$ ,  $\lambda_z$  and  $k'$ . The array of electrodes was lowered into the spinal cord either to a depth of 250–350  $\mu\text{m}$  from the dorsal spinal surface for measurements in dorsal horn gray matter (layers 3–5)<sup>13</sup> or from the ventral surface to a depth of 200–300  $\mu\text{m}$  for measurements in spinal cord white matter. At the conclusion of the experiments, the spinal cords were cut transversally at the level of the microelectrode insertion and inspected under a stereomicroscope to ensure that the measurements were made from white matter.

## Results

We previously reported that a decrease in  $\alpha$  in rat cortex and corpus callosum during postnatal development occurred faster in gray than in white matter.<sup>8,14,15</sup> In the present study, we confirmed this finding in spinal cord. Diffusion parameters in spinal cord gray and white matter were studied during the first three postnatal weeks (Fig. 2). Our measurements show that  $\alpha$  in dorsal horn gray matter decreased at the end of the first postnatal week to about 0.22 and then remained unchanged. Tortuosity  $\lambda$  increased and non-specific uptake  $k'$  decreased with time; however, these changes occurred more slowly and gradually than did the decrease in the ECS volume fraction  $\alpha$ , reaching their final values in the second and third postnatal week, respectively (Fig. 2). This suggests that the increase in  $\lambda$  may be related to either an increased number of cellular

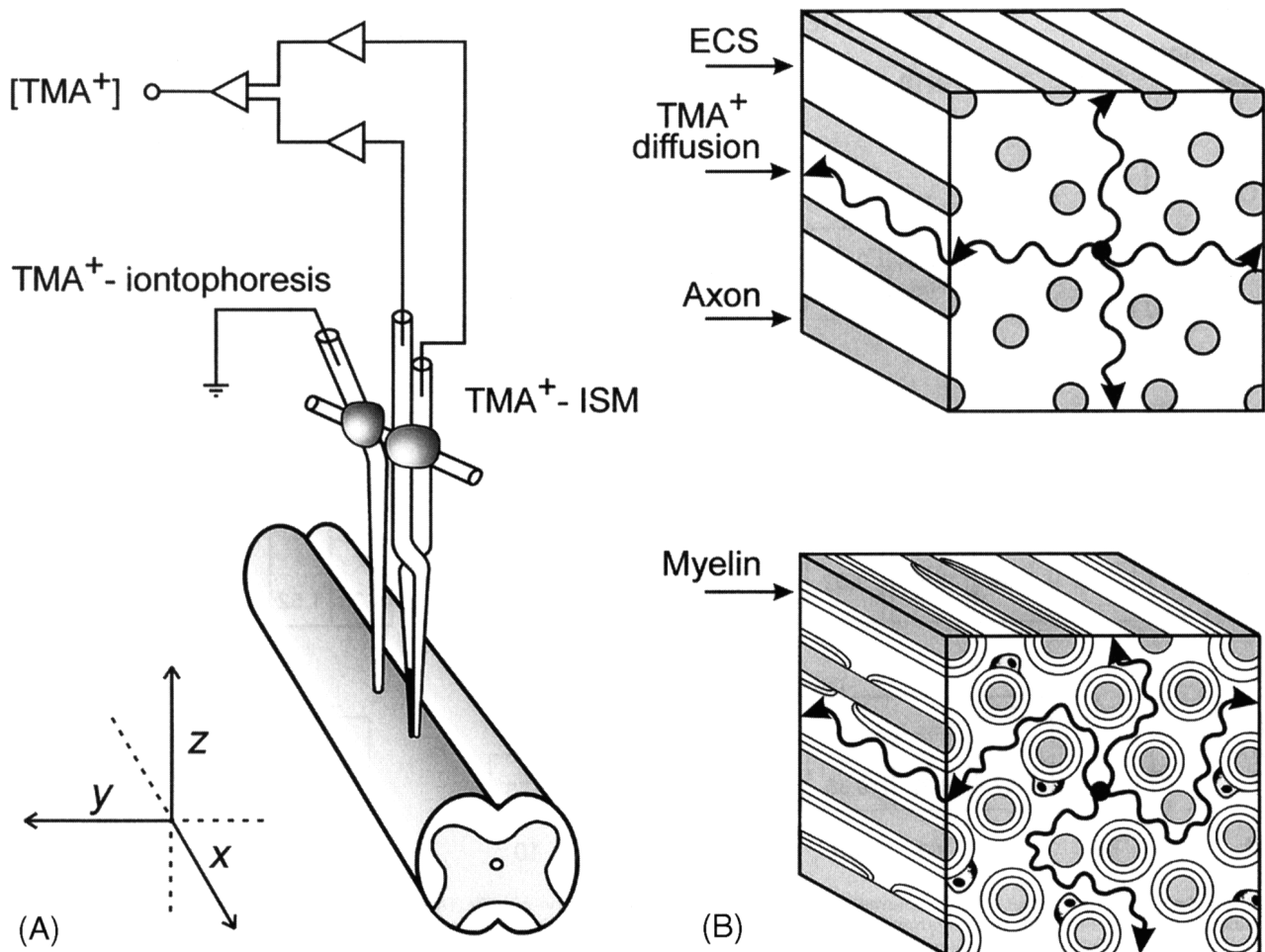


FIG. 1. Experimental setup and scheme of iso- and anisotropic  $\text{TMA}^+$  diffusion. Left: the experimental arrangement. (A)  $\text{TMA}^+$ -selective double-barreled ion-selective microelectrode (ISM) was glued to an iontophoresis microelectrode. The separation between electrode tips was 100–220  $\mu\text{m}$ . For measurements along the  $z$  axis, the iontophoresis pipette tip was lowered 100–220  $\mu\text{m}$  below the tip of the ISM. When the electrode array was inserted into the spinal cord and the iontophoretic current applied, the diffusion curve resulting from the increase in  $\text{TMA}^+$  concentration could be measured in the  $x$ ,  $y$  or  $z$  axis. (B) Diffusion in the extracellular space of unmyelinated and myelinated white matter. Extracellular diffusion in a direction perpendicular to the orientation of the axons (i.e. around the axons) is compromised by myelin sheaths. The scheme demonstrates an increased anisotropy as myelination progresses.

processes, extensive gliogenesis, changes in the extracellular matrix, or all of these events.

Figure 3A–D shows that the diffusion curves obtained in the spinal cord have a greater amplitude than those in agar gel because the same amount of  $\text{TMA}^+$  released from the iontophoretic electrode results in a greater increase in  $\text{TMA}^+$  concentration in nervous tissue than in free medium due to the restricted ECS available for diffusion.  $\text{TMA}^+$  diffusion curves in the spinal cord also rose more slowly than those in agar gel (Fig. 3A–D), reflecting the reduction of the  $\text{TMA}^+$  apparent diffusion coefficient (ADC) in nervous tissue and therefore an increase in  $\lambda$ .

$\text{TMA}^+$  diffusion curves recorded from dorsal horn gray matter and from white matter revealed distinct diffusion properties in these structures as early as the first postnatal week (Fig. 2). ECS volume fraction in

white matter was higher at the first postnatal week than that in gray matter, and it significantly decreased in the second postnatal week, i.e. during the period of extensive myelination.<sup>16</sup> While the same diffusion curves were recorded from the  $x$ ,  $y$  and  $z$  axes within the dorsal horn, different diffusion curves were recorded along each of the axes in the white matter, indicating that spinal cord white matter is substantially anisotropic (Fig. 3). Figures 2 and 3 show that preferential diffusion in white matter occurred along the myelinated axons. Diffusion in spinal cord is affected by  $\alpha$  and  $\lambda$ , as is readily apparent from an inspection of the time-course and amplitude of the  $\text{TMA}^+$  diffusion curves (Fig. 3). The non-specific linear uptake,  $k'$ , is, like  $\alpha$ , a scalar quantity, and therefore has a single value in all three axes. The uptake significantly increased as the animals aged (Fig. 2).

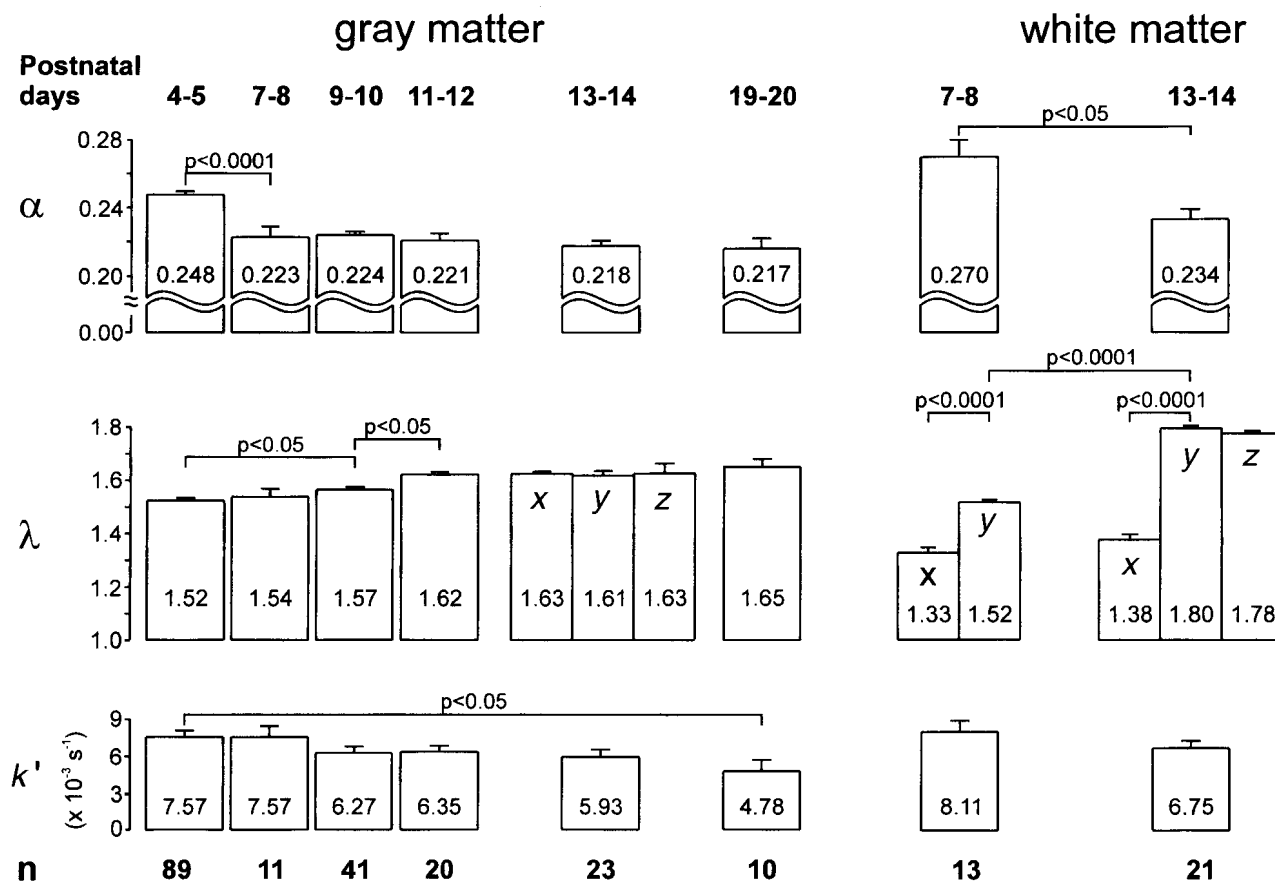


FIG. 2. Comparison of mean  $\pm$  s.e.m. volume fraction ( $\alpha$ ), tortuosity ( $\lambda$ ) and non-specific TMA<sup>+</sup> uptake ( $k'$ ) in gray and white matter of the isolated rat spinal cord. Diffusion parameters were studied in gray matter at age P4–20 and in white matter at ages P7–8 and P13–14.  $n$  is the number of animals in each group. Diffusion in gray matter was isotropic, and therefore only a single mean value of  $\lambda$  is given, except at P13–14. In white matter, anisotropic diffusion was found, and the mean values for  $\lambda$  measured along the axons ( $x$  axis) and perpendicular to the axons ( $y$  axis and  $z$  axis) are given. At P7–P8 the white matter is too narrow in the  $z$  axis to allow for diffusion measurements.

The three-dimensional pattern of diffusion away from a point source can be illustrated by constructing iso-concentration spheres (isotropic diffusion) and ellipsoids (anisotropic diffusion) for extracellular TMA<sup>+</sup> concentration. The surfaces in Fig. 3E–G represent the locations where TMA<sup>+</sup> concentration first reached 1 mM, 10 s after the initiation of an 80 nA iontophoresis current. The value of  $r$  for which extracellular TMA<sup>+</sup> concentration was equal to 1 mM was found graphically by solving the appropriate equations governing diffusion in nervous tissue.<sup>8–10</sup> We used the mean values for  $\alpha$ ,  $\lambda_x$ ,  $\lambda_y$ ,  $\lambda_z$  and  $k'$  given in Fig. 2, together with the following parameters:  $D = 9.428 \times 10^{-6} \text{ cm}^2 \text{ s}^{-1}$  at 20°C,  $n = 0.370$ . The three-dimensional plots were then generated from the expression  $z = (r^2 - x^2\lambda_x^2 - y^2\lambda_y^2)^{1/2}/\lambda_z$  derived from the definition of  $r$ .<sup>7</sup> The single value for  $r$ , which describes the equivalent sphere determined by this procedure, was 27  $\mu\text{m}$  for agar gel and 96  $\mu\text{m}$  for gray matter. The spherical surface reflects the ability of particles to diffuse equally along the  $x$ ,  $y$  and  $z$

axes. The tiny sphere representing diffusion in agar gel (Fig. 3E) shows the dramatic difference between a free medium and constrained diffusion in the spinal cord. The larger the ECS volume fraction, the smaller the sphere. In white matter  $r_x$ ,  $r_y$  and  $r_z$  describing the equivalent ellipsoid were 114, 87 and 88  $\mu\text{m}$ , respectively. The ellipsoidal surface in Fig. 3G reflects the different abilities of substances to diffuse along the  $x$ ,  $y$  and  $z$  axes in myelinated white matter.

### Discussion

To characterize the anisotropy of mammalian extracellular space (ECS), we have studied extracellular diffusion in rat dorsal horn gray matter and ventral white matter. These regions were selected because the axons in the white matter are myelinated and oriented in parallel, and therefore should constrain diffusion. On the other hand, Rexed laminae III to V of the dorsal horn are rich with cell bodies, dendrites and axons which have no preferential orientation, and

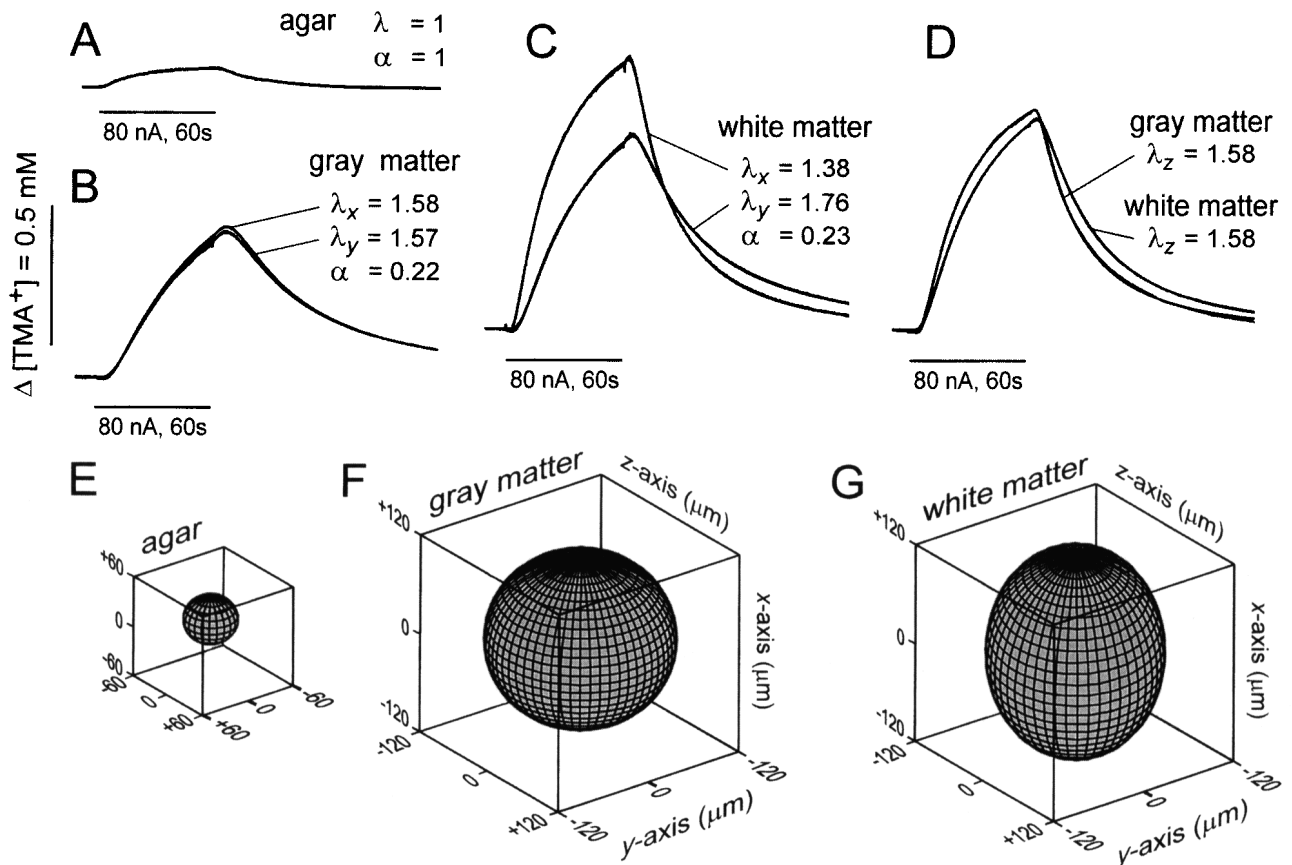


FIG. 3. Representative records obtained in agar gel, spinal dorsal horn gray matter and white matter (ventral funiculus) in the *x* axis (along the axons) and in the *y* and *z* axes (across the axons). Recordings are from animals at P14. The values for volume fraction ( $\alpha$ ) and tortuosity ( $\lambda$ ) are shown with each curve. (A) Measurements in agar gel. (B) Gray matter: in the *x* and *y* axes the same microelectrode array spacing was used ( $210 \mu\text{m}$ ) and  $n = 0.343$ . (C) White matter: in the *x* and *y* axes the microelectrode array spacing was  $164 \mu\text{m}$  and  $n = 0.368$ . (D) Gray and white matter: in the *z* axis, the microelectrode array spacing in gray matter was  $145 \mu\text{m}$ ,  $n = 0.345$  and in white matter  $168 \mu\text{m}$ ,  $n = 0.424$ . The shape and amplitude of the diffusion curves reflect different diffusion coefficients along each of the selected axes. Both diffusion curves in (B), (C) and (D) were recorded in the same animal. (E–G) Diffusion spheres were constructed from the diffusion curves in agar, gray and white matter: iso-concentration surfaces for a  $1 \text{ mM TMA}^+$  concentration contour  $10 \text{ s}$  after the onset of an  $80 \text{ nA}$  iontophoretic pulse revealed spherical (isotropic) diffusion in agar (E) and in gray matter (F), and ellipsoidal (anisotropic) diffusion in white matter (G). The surfaces were generated as described in the text using the mean values for  $\alpha$ ,  $\lambda_x$ ,  $\lambda_y$ ,  $\lambda_z$  and  $K$  given in Fig. 2.

therefore the diffusion might be rather isotropic. Indeed, our data revealed that diffusion in spinal dorsal horn is isotropic, although anisotropy in gray matter was previously reported in some brain regions.<sup>7,17</sup> To determine whether axon fiber orientation and/or myelination plays a crucial role in white matter anisotropy, we investigated rats at two different ages. At P1–P6 the white matter is too narrow to allow study of diffusion between electrodes separated by  $100\text{--}220 \mu\text{m}$ . However, between P7 and P14 extensive myelination takes place,<sup>16</sup> and this corresponds well with our findings that between P7 and P14 anisotropy substantially increased. Our data therefore show that diffusion in the ECS of myelinated axon bundles is largely anisotropic, with preferential diffusion along the axons. Similar findings using the TMA<sup>+</sup> method were recently reported in myelinated corpus callosum between P13 and P20.<sup>8</sup> In this study, the diffusion in unmyelinated corpus

callosum at P4–P12 was isotropic. Anisotropy was also found in the neostriatum of adult rats where the distribution of fluorescent-labelled dextran has been used.<sup>17</sup> Our model shown in Fig. 1, which is based on present TMA<sup>+</sup> diffusion data and immunohistochemical studies,<sup>16,18</sup> shows that the beginning of myelination results in the maturation of a structural component which does have directionality, and hence the tissue becomes increasingly anisotropic.

Structural anisotropy in some regions of the brain has also been inferred from impedance measurements and MRI. Neither impedance<sup>19</sup> nor MRI<sup>20</sup> can, however, distinguish between the intra- and extracellular compartments, and therefore these studies could not confirm the extent of anisotropy in the extracellular space.

Tortuosity is a geometrical parameter that incorporates many factors which we presently cannot determine as separate entities. These might include

membrane barriers, including neuronal and glial processes, myelin sheaths; macromolecules including the molecules of the extracellular matrix; molecules with fixed negative surface charges; extracellular space size and pore geometry. Our recent studies support a role for geometrical constraints, since an increase in tortuosity accompanied astrogliosis evoked by radiation injury,<sup>11</sup> astrogliosis and myelination in grafted tissue<sup>21</sup> and a rise in the macromolecular content of the extracellular fluid.<sup>3,22</sup>

In previous studies we showed that in adult rat spinal cord, ECS volume fraction and tortuosity are 0.20 and 1.62 in dorsal horn gray matter and 0.18 and 1.56 in white matter, respectively.<sup>23,24</sup> In the cortex and corpus callosum,  $\alpha$  decreases in the first 3 postnatal weeks to about one half of its size at P2–3 while the tortuosity is essentially unchanged.<sup>11,14</sup> Our measurements, however, were made only along the  $x$  axis and were correct only if one assumes that the diffusion in this developmental period is isotropic. Although this is the case in cortical gray matter, the present experiments revealed substantial anisotropy in white matter. Two distinct age groups, P7–8 and P13–14, were selected for comparison and the results are presented in Fig. 2. At P13–14, a significant difference ( $p < 0.0001$ ) was found between  $\lambda_x$  and  $\lambda_y$  values and between  $\lambda_x$  and  $\lambda_z$  values. This time-course of tortuosity increase across the axon fibers correlates with white matter myelination.<sup>16</sup> The importance of the tortuosity increase due to myelination is supported by recent similar findings in the corpus callosum where diffusion was also studied in three axes.<sup>8</sup> Our model in Fig. 1 shows that during development, diffusion along the axons might be less hindered since the size of the space between axons is still large enough not to significantly affect TMA<sup>+</sup> diffusion. In this more detailed study, tortuosity also significantly increased with development in gray matter, presumably due to advanced maturation of astrocytes and oligodendrocytes.

The ECS represents the pathway for extrasynaptic transmission and for intercellular, particularly neuron–glia, communication. ECS diffusion parameters, including anisotropy, may help to limit the diffusion of transmitters to regions occupied by their high affinity receptors, located extrasynaptically and often coupled to G-proteins.<sup>25</sup> In addition, ECS diffusion parameters affect the diffusion of ions,

metabolites and neuroactive substances during physiological and pathological states. The anisotropy of the ECS in spinal cord, corpus callosum,<sup>8</sup> cerebellum,<sup>7</sup> hippocampus (Syková and Mazel, unpublished data) and in neostriatum<sup>17</sup> may allow for some specificity and for new modes of extrasynaptic transmission.

## Conclusion

Evidence has been provided for heterogeneous diffusion in spinal cord gray and white matter during postnatal development. In both gray and white matter, extracellular space volume fraction decreases, tortuosity increases and non-specific uptake decreases during the first two postnatal weeks. The diffusion in gray matter was found to be isotropic, while in white matter the diffusion anisotropy increases during myelination in the second postnatal week. Our data show that the preferential diffusion pathways in spinal cord white matter are along the myelinated axon fibres.

## References

1. Agnati LF, Zoli M, Stromberg I and Fuxe K. *Neurosci* **69**, 711–726 (1995).
2. Syková E. *Neuroscientist* **3**, 334–347 (1997).
3. Tao L and Nicholson C. *Neuroscience* **75**, 839–847 (1996).
4. Berger T, Muller T and Kettenmann H. *Perspect Dev Neurobiol* **2**, 347–356 (1995).
5. Fuxe K and Agnati LF. *Volume Transmission in the Brain: Novel Mechanisms for Neural Transmission*. New York: Raven Press, 1991.
6. Peters A and Palay SL. *J Anat* **99**, 419 (1965).
7. Rice ME, Okada YC and Nicholson C. *J Neurophysiol* **70**, 2035–2044 (1993).
8. Voříšek I and Syková E. *J Neurophysiol* **78**, 912–919 (1997).
9. Rice ME and Nicholson C. *J Neurophysiol* **65**, 264–272 (1991).
10. Nicholson C and Phillips JM. *J Physiol (Lond)* **321**, 225–257 (1981).
11. Syková E, Svoboda J, Šimonová Z et al. *Neurosci* **70**, 597–612 (1996).
12. Voříšek I and Syková E. *J Cerebr Blood Flow Metab* **17**, 191–203 (1997).
13. Molander C and Grant G. Spinal cord cytoarchitecture. In: Paxinos G, ed. *The Rat Nervous System*. San Diego: Academic Press, 1995.
14. Lehmenkühler A, Syková E, Svoboda J et al. *Neuroscience* **55**, 339–351 (1993).
15. Chvátal A, Berger T, Voříšek I et al. *J Neurosci Res* **49**, 98–106 (1997).
16. Hamano K, Iwasaki N, Takeya T and Takita H. *Dev Brain Res* **93**, 18–22 (1996).
17. Bjelke B, England R, Nicholson C et al. *NeuroReport* **6**, 1005–1009 (1995).
18. Bjartmar C. *Neurosci Lett* **216**, 85–88 (1996).
19. Garden-Medwin AR. *Neurosci Res Prog Bull* **18**, 208–226 (1980).
20. Moseley ME, Cohen Y, Kucharczyk J et al. *Radiology* **176**, 439–445 (1990).
21. Roitbak T, Mazel T, Šimonová Z et al. *Eur J Neurosci (Suppl)* **9**, 37 (1996).
22. Prokopová, Nicholson C and Syková E. *Physiol Res* (in press).
23. Syková E, Svoboda J, Polák J and Chvátal A. *J Cerebr Blood Flow Metab* **14**, 301–311 (1994).
24. Šimonová Z, Svoboda J, Orkand P et al. *Physiol Res* **45**, 11–22 (1996).
25. Gilman AG. *Annu Rev Biochem* **56**, 615–649 (1987).

ACKNOWLEDGEMENTS: Supported by grants GACR 309/96/0884, GACR 307/96/K226 and IGA MZ 3423-3, GACR 309/97/K048.

Received 20 June 1997;  
accepted 23 August 1997